

AD-A092 407

NAVAL POSTGRADUATE SCHOOL MONTEREY CA
EXPERIMENTAL STUDY OF CONTRAST UTILIZING A VIDICON.(U)
JUN 80 R W HAVEL

F/G 9/1

UNCLASSIFIED

NL

(OF)
2/3/2007

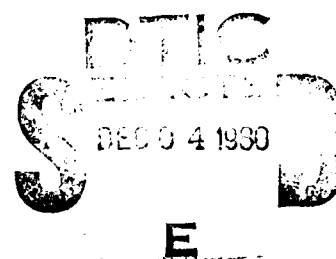
END
DATE
FILMED
61-2
DTIC

LEVEL II

②

NAVAL POSTGRADUATE SCHOOL
Monterey, California

AD A092407



THESIS

EXPERIMENTAL STUDY OF CONTRAST
UTILIZING A VIDICON

by

Richard William Havel

June 1980

Thesis Advisor:

E. C. Crittenden Jr.

Approved for public release; distribution unlimited

DDC FILE COPY

80 1-01

Unclassified

SECURITY CLASSIFICATION OF THIS PAGE (When Data Entered)

REPORT DOCUMENTATION PAGE		READ INSTRUCTIONS BEFORE COMPLETING FORM
1. REPORT NUMBER	2. GOVT ACCESSION NO.	3. RECIPIENT'S CATALOG NUMBER
	AD-A092407	(9)
4. TITLE (and Subtitle)		5. TYPE OF REPORT & PERIOD COVERED
(6) EXPERIMENTAL STUDY OF CONTRAST UTILIZING A VIDICON.		Master's Thesis, June 1980
7. AUTHOR(s)		8. PERFORMING ORG. REPORT NUMBER
(10) Richard William/Havel		
9. PERFORMING ORGANIZATION NAME AND ADDRESS		10. PROGRAM ELEMENT, PROJECT, TASK AREA & WORK UNIT NUMBERS
Naval Postgraduate School Monterey, California 93940		
11. CONTROLLING OFFICE NAME AND ADDRESS		12. REPORT DATE
Naval Postgraduate School Monterey, California 93940		June 1980
13. MONITORING AGENCY NAME & ADDRESS (if different from Controlling Office)		14. NUMBER OF PAGES
Naval Postgraduate School Monterey, California 93940		61
		15. SECURITY CLASS. (of this report)
		Unclassified
		16. DECLASSIFICATION/DOWNGRADING SCHEDULE
17. DISTRIBUTION STATEMENT (of this Report)		
Approved for public release; distribution unlimited		
18. DISTRIBUTION STATEMENT (of the abstract entered in Block 20, if different from Report)		
19. SUPPLEMENTARY NOTES		
20. KEY WORDS (Continue on reverse side if necessary and identify by block number)		
contrast vidicon visibility		
21. ABSTRACT (Continue on reverse side if necessary and identify by block number)		
<p>A commercial multi-purpose closed circuit television camera system with a vidicon image tube was studied to determine its capability for measurement of contrast and visibility. A single line of the scan from the camera video output was extracted and examined with an oscilloscope. A derivation of system response was made and a comparison performed with laboratory data. Calibration of the field of view, for one particular television pick-up tube, revealed nonuniformities making resolution of 2 percent</p>		

DD FORM 1473
(Page 1)

EDITION OF 1 NOV 68 IS OBSOLETE
S/N 0102-016-6601

Unclassified
SECURITY CLASSIFICATION OF THIS PAGE (When Data Entered)

251450

20. cont.:

contrast difficult. Useful resolution results are expected with improvement of the pick-up tube or with employment of digital processing techniques.

Accession For	
REIS CH 21	<input checked="" type="checkbox"/>
LDC TAB	<input type="checkbox"/>
Unannounced	<input type="checkbox"/>
Justified	<input type="checkbox"/>
Date	
Time	
Initials	
Special	
Dist	
A	

DD Form 1473
S/N 0102-014-6601

Unclassified
SECURITY CLASSIFICATION OF THIS PAGE/When Data Entered

Approved for public release; distribution unlimited

Experimental Study of Contrast
Utilizing a Vidicon

by
Richard William Havel
Lieutenant Commander, United States Navy
B.S., University of Notre Dame, 1969

Submitted in partial fulfillment of the
requirements for the degree of

MASTER OF SCIENCE IN PHYSICS

from the

NAVAL POSTGRADUATE SCHOOL
June 1980

Author

Approved by:

Richard W. Havel

E. L. Brittenden, Jr.

Thesis Advisor

A. W. Cooper

Second Reader

J. M. Dyer

Chairman, Department of Physics and Chemistry

William M. Jolley

Dean of Science and Engineering

ABSTRACT

A commercial multi-purpose closed circuit television camera system with a vidicon image tube was studied to determine its capability for measurement of contrast and visibility. A single line of the scan from the camera video output was extracted and examined with an oscilloscope. A derivation of system response was made and a comparison performed with laboratory data. Calibration of the field of view, for one particular television pick-up tube, revealed nonuniformities making resolution of 2 percent contrast difficult. Useful resolution results are expected with improvement of the pick-up tube or with employment of digital processing techniques.

TABLE OF CONTENTS

I.	INTRODUCTION-----	8
II.	THEORY-----	9
	A. CONTRAST, VISIBILITY AND ATMOSPHERIC EFFECTS-----	9
	B. VIDICON-----	13
	C. VIDEO OUTPUT-----	16
III.	SYSTEM COMPONENTS-----	20
	A. THE CAMERA-----	20
	B. THE ELECTRONICS-----	24
	C. THE CALIBRATION UNIT-----	25
IV.	PROCEDURE AND RESULTS-----	30
	A. PRELIMINARY-----	30
	B. CALIBRATION-----	36
	C. TYPICAL SCENE-----	48
V.	CONCLUSIONS AND AREAS FOR FURTHER STUDY-----	50
	APPENDIX A OPERATING CHARACTERISTICS OF CAMERA-----	52
	APPENDIX B OSCILLOSCOPE SETTINGS-----	54
	APPENDIX C DATA-----	55
	BIBLIOGRAPHY-----	60
	INITIAL DISTRIBUTION LIST-----	61

LIST OF FIGURES

1. Vidicon Tube-----	14
2. Photoconductive Layer-----	17
3. Vidicon Response-----	17
4. System Arrangement-----	21
5. The Camera-----	23
6. The Electronics-----	23
7. The Calibration Tube-----	26
8. Calibration Tube (Camera End)-----	28
9. Calibration Tube (Side View)-----	28
10. Calibration Tube (Source End)-----	29
11. Screen and Filter Trays-----	29
12. Laboratory Object Scene-----	31
13. Lab Object - Entire Scan-----	32
14. Lab Object - 8 Lines-----	32
15. Lab Object - Single Line-----	33
16. Single Line Sketch-----	33
17. Lateral Monitor-Scope Correlation-----	35
18. Vertical Monitor-Scope Correlation-----	35
19. Screen w/o Filter - Track A-----	37
20. Screen w/o Filter - Track B-----	37
21. Screen with Filter - Track A-----	38
22. Screen with Filter - Track B-----	38

23. Monitor - Screen with Filters-----	40
24. Signal of Monitor Scene - Track A-----	40
25. Deflection vs Slit No. - Track A-----	41
26. Deflection vs Slit No. - Track B-----	41
27. Output from Single Slit-----	42
28. Deflection Mean (Column) vs Lateral Monitor Position-----	44
29. Deflection Mean (Row) vs Vertical Monitor Position-----	44
30. Deflection vs Transmittance-----	46
31. Deflection vs Neutral Density No.-----	46
32. $\ln(1-fD)$ vs Transmittance - Track A-----	47
33. $\ln(1-fD)$ vs Transmittance - Track B-----	47
34. Photograph of Actual Scene-----	49
35. Output from Horizon Area of Actual Scene-----	49
36. Image Tube Spectral Response-----	53

I. INTRODUCTION

The determination and prediction of visibility is basic to a variety of endeavors ranging from recreation to safety to warfare; its value ranges from satisfying the curiosity to absolute necessity for survival. Visibility, as such, is a very subjective term depending critically upon the recognition capabilities of the observer under the prevailing conditions; it can be determined once the apparent contrast of an object against its background is measured and the effects of the intervening atmosphere applied.

Instrumentation which directly measures apparent contrast without the involvement of the human factor is a requirement for accurate determination of visibility. Many devices have been designed specifically for this task and its corollary, the study of the intervening atmosphere. The intent of this project is to examine the capabilities of an instrument not specifically designed for this task - a television camera using a vidicon tube.

II. THEORY

A. CONTRAST, VISIBILITY AND ATMOSPHERIC EFFECTS

Most of the information received through the eyes depends on the perception of differences in luminance (or brightness) and chromaticity (color) between different areas in the field of view. For the purposes of this experiment luminance differences ("black and white") only were considered. An object is distinguished or recognized when its brightness differs from that of the surroundings.

Assuming that an isolated object is surrounded by a uniform and fairly extensive background, the object-background contrast has been defined in a variety of ways depending upon the application (e.g. $C = (B-B')/(B + B')$, $C = (B-B')/B$, $C = (B-B')/B'$, and $C = B/B'$). For this project, the definition most commonly found in the reference material [1,3,4,8, 9,] has been adopted:

$$C = \frac{B-B'}{B'} \quad (1)$$

where B and B' are the luminances of the object and the background respectively. The range of C is from -1 to ∞ , where a dark object viewed against the daytime sky will exhibit a negative value and a light source against the night sky a positive value.

Duntley [3] has shown that the contrast between a pair of objects varies exponentially with distance due to atmospheric attenuation. If B_o is the inherent luminance of an object when seen from very close range and B_r is the apparent luminance of an object seen from a distance r then Duntley stated that

$$B_r - B'_r = (B_o - B'_o) \exp(-\beta R) \quad (2)$$

where R is the range from the object and β the atmospheric attenuation coefficient.

Accordingly, the inherent and apparent contrasts may also be defined (as per Eq. (1)) as

$$C_o = \frac{B_o - B'_o}{B'_o} \quad (3)$$

and

$$C_r = \frac{B_r - B'_r}{B'_r} \quad (4)$$

By substituting Eqs. (2) and (3) in Eq. (4) the following general expression for the law of contrast reduction results:

$$C_r = \frac{B'_o}{B'_r} C_o \exp(-\beta R) \quad (5)$$

For a horizontal line of sight, the horizon luminance is constant as one moves toward or away from the object (because the distance to the horizon never changes and its apparent luminance is always its inherent luminance);

therefore $B'_0 = B'_r$ and

$$C_r = C_0 \exp(-BR) \quad (6)$$

Equation (6) expresses the attenuation of contrast for objects of any inherent contrast.

A perfect black object will have an inherent contrast of -1 regardless of its background and its apparent contrast reduces to

$$C_r = -\exp(-BR) \quad (7)$$

The response of the eye to various stimuli is complex; Weber's Law states that "The increase of stimulus necessary to produce a just perceptible increment of sensation bears a constant ratio to the whole stimulus." For this experiment, daylight conditions only were considered, and for vision the "just perceptible increment of sensation" is known as the visual threshold of perception. This threshold ϵ is defined as

$$\epsilon = \frac{\Delta L}{L} \quad (8)$$

where ΔL is the least perceptible increment of luminance between two objects.

Figure 5.2 of Middleton [9] shows curves for threshold of brightness-contrast as a function of field luminance for different stimulus sizes and 50 percent detection; Figure 1.10 of McCartney [8] shows curves for luminance-contrast. In each figure, the lower curves (larger stimuli) approach

a threshold of contrast of $\epsilon = 0.02$ in the limit as background conditions get very light. Although this liminal contrast is not constant at 0.02 it is convenient to assume so for visual range calculations and atmospheric studies.

Visual range is defined [6] as "the distance under daylight conditions, at which the apparent contrast between a specified type of target and its background (horizon sky) becomes just equal to the threshold contrast of an observer."

Thus by applying Eq. (6) and the above definition the visual range V may be specified by

$$\epsilon = C_o \exp(-\beta V) \quad (9)$$

or

$$V = \frac{1}{\beta} \ln |C_o / \epsilon| \quad (10)$$

By specifying a "black object" where $C_o = -1$ and the threshold contrast $\epsilon = 0.02$, the meteorological range may be determined

$$V_m = \frac{1}{\beta} \ln |1/0.02| = \frac{3.912}{\beta} \quad (11)$$

and conversely

$$\beta = \frac{3.912}{V_m} \quad (12)$$

and Eq. (6) becomes

$$C_r = C_o \exp\left(-\frac{3.912R}{V_m}\right) \quad (13)$$

Under stable conditions and for horizontal directions, V_m is constant; then range and apparent contrast are related by Eq. (13) if C_o can be determined.

In summary, range, contrast, and the attenuation coefficient are related; knowledge of two determines the third.

A variety of instruments have been designed to use the foregoing for measurements of visibility. The comparison photometer and the nephelometer both measure the apparent contrast at a known distance and apply Eq. (13). Other instruments, broadly classified as telephotometers, measure light at a distance. An example is the transmissometer which calculates β by measuring the attenuation of light over a fixed short distance, assumes that it is indicative of the atmosphere in general, and predicts V_m ; the Runway Visibility Range (RVR) meter is a transmissometer used to predict ranges at the runway, normally under 6000 feet.

These instruments were all designed for the task of quantitative contrast and visibility determination; the purpose of this experiment was to use an instrument not so designed.

B. VIDICON

The vidicon (see Fig. 1) is a pick-up tube wherein light impinges on a photoconductive target which is electronically scanned to produce a video signal. Specifically it consists of an electron gun, focusing anode, anode mesh which is a decelerating grid, and a glass faceplate which

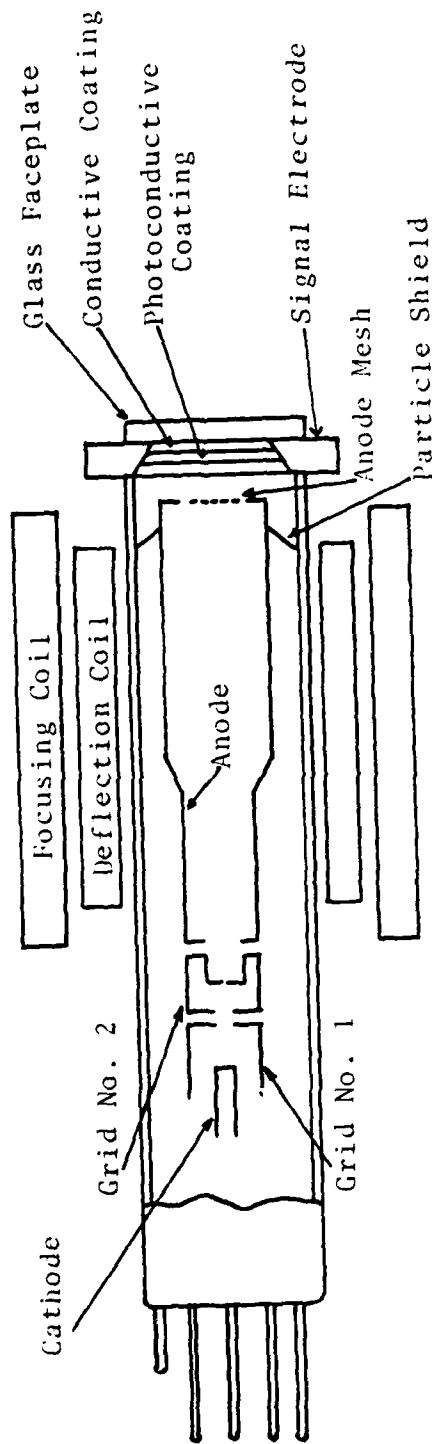


Fig. 1. Vidicon Tube

is covered on its inside surface with a thin transparent conductive coating; over this layer is deposited a film of photoconductive material. The conductive coating is connected to the target or signal output and maintained at a small (adjustable) positive potential.

The photoconductive coating is essentially an insulator in the dark, but conductive when illuminated. Illumination incident on the conductive coating increases its conductivity in the areas illuminated; at these points charge flows to the back side of the coating, making it positive. The scanning electron beam resets the spot to zero causing a voltage pulse in the layer which is sensed as a "video" signal. When the photoconductive coating is dark, its resistance is high and charge accumulates on the back surface (from the scanning beam) as in a capacitor. Where it is light, target current flows in proportion to the amount of light striking the surface. On the following scan, electrons are deposited in the discharged regions causing the current flow which in turn causes a voltage signal across a load resistor.

The video signal represents the amount of light that has fallen on that particular spot in the layer since the previous scan. Timing allows the interrogation of each spot in the layer by the raster and the video signal is formed.

Focusing of the electron beam is done by a magnetic field which is parallel to the axis of the tube. Deflection is accomplished by means of magnetic fields perpendicular to the axis of the tube formed by external coils.

Each photoconductor element may be considered a capacitor with one plate connected to the positive target voltage and the other plate grounded. Each element contains internal resistance inversely proportional to the amount of illumination striking it. Increasing or decreasing the target voltage or the illumination on the tube will cause a corresponding increase or decrease in the video output signal.

C. VIDEO OUTPUT

In order to interpret the output of the vidicon the following analysis was made.

It was assumed that the response of one photoconductive element of length ℓ and area A illuminated by I (Fig. 2) is that of a resistive-capacitive circuit initially at a potential V_0 decaying exponentially in time (Fig. 3). If R is the resistance, C the capacitance, and σ the conductivity of the element, then

$$V = V_0 \exp(-t/RC) \quad (14)$$

$$\text{but } R = \frac{1}{\sigma} \frac{\ell}{A} = \frac{1}{a\sigma} \quad \text{Where } a = \frac{A}{\ell} = \text{constant}$$

$$\text{and } t = 1/30 \text{ sec} = \text{constant}$$

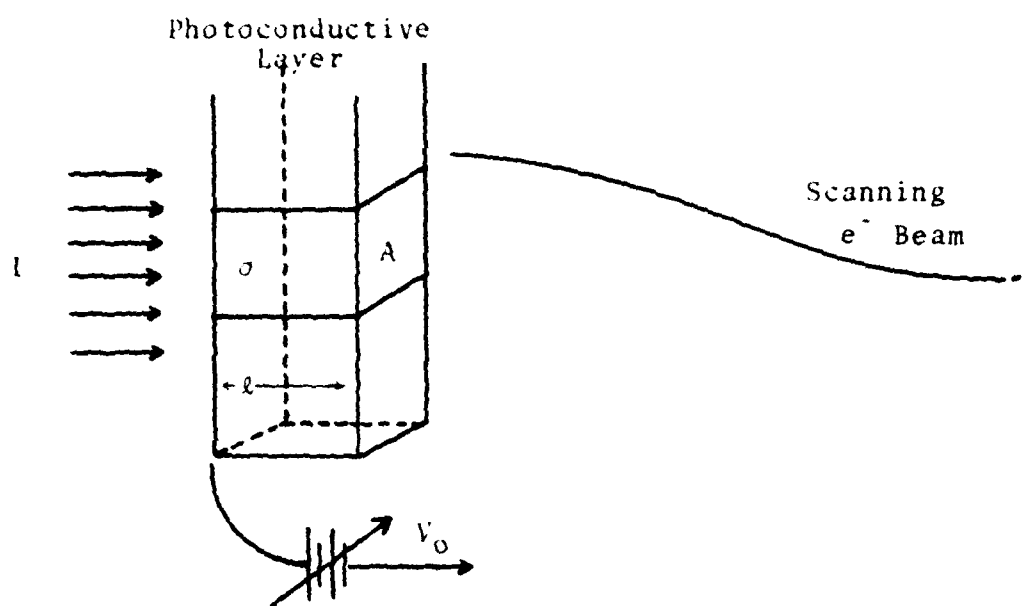


Fig. 2. Photoconductive Layer

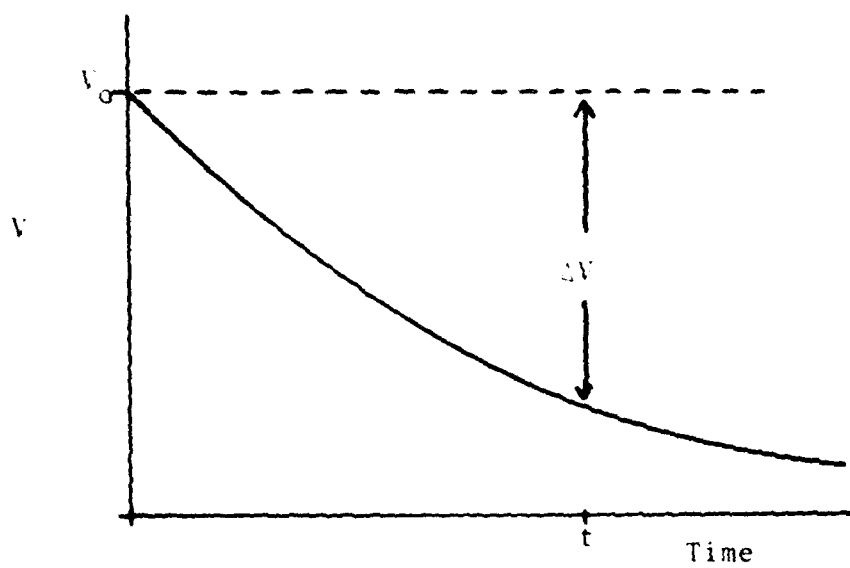


Fig. 3. Vidicon Response

and let $b = \frac{ta}{c} = \text{constant}$

then $V = V_0 \exp(-b\sigma)$ (15)

It was assumed that the conductivity of the element was linearly dependent on the illumination:

$$\sigma = \sigma_0 + dI \quad (16)$$

where σ_0 and d were constants; therefore Eq. (15) became

$$V = V_0 \exp(-b(\sigma_0 + dI)) \quad (17)$$

consequently,

$$\Delta V = V_0 - V = V_0 (1 - \exp(-b(\sigma_0 + dI))) \quad (18)$$

and $1 - \frac{\Delta V}{V_0} = \exp(-b(\sigma_0 + dI))$

or $\ln(1 - \frac{\Delta V}{V_0}) = -b\sigma_0 - eI \quad (19)$

where $e = bd = \text{constant}$

It was then assumed that the deflection (D) of an oscilloscope trace connected to the video output was linear in ΔV ;

then $\frac{\Delta V}{V_0} = fD \quad (20)$

where V_0 and f are constants

then $\ln(1 - fD) = -b\sigma_0 - eI \quad (21)$

Furthermore, it was assumed that $I = TI_0$ where T was the transmittance and I_0 the original intensity.

Redefining constants

$$\sigma^* = -b\sigma_0$$

$$g = -eI_0$$

Eq. (21) then became

$$\ln(1-fD) = \sigma^* + gT \quad (22)$$

which implied that once a suitable f was found, the term $\ln(1-fD)$ was linear in T . Part of this experiment was thus to determine f , g and σ^* so that Eq. (22) was valid. A comparison between experimental data and this theory was performed in Section IV. B of this report.

III. SYSTEM COMPONENTS

The system chosen to study contrast consisted of a closed circuit television camera and monitor, an active bandpass filter, an oscilloscope, and a calibration unit. The calibration unit was locally designed and fabricated; the remaining elements were off-the-shelf items available at the Naval Postgraduate School, and were set up as shown in Fig. 4.

A. THE CAMERA

The camera used was a Diamond Model ST-1 Vidicon Camera with an Ampex TV Zoom (22.5-90mm.) Lens and a CONRAC II nine inch monitor. This camera was designed for a wide variety of general closed circuit television applications; as supplied it had an all electronic light compensation system designed to automatically maintain a high quality picture without readjustment under a range of light conditions. The Vidicon 7735A tube was designed for televising live scenes in educational, industrial and other closed-circuit television applications where broadcast quality scene reproduction was not essential. The spectral response curve for this tube was centered at approximately 5500

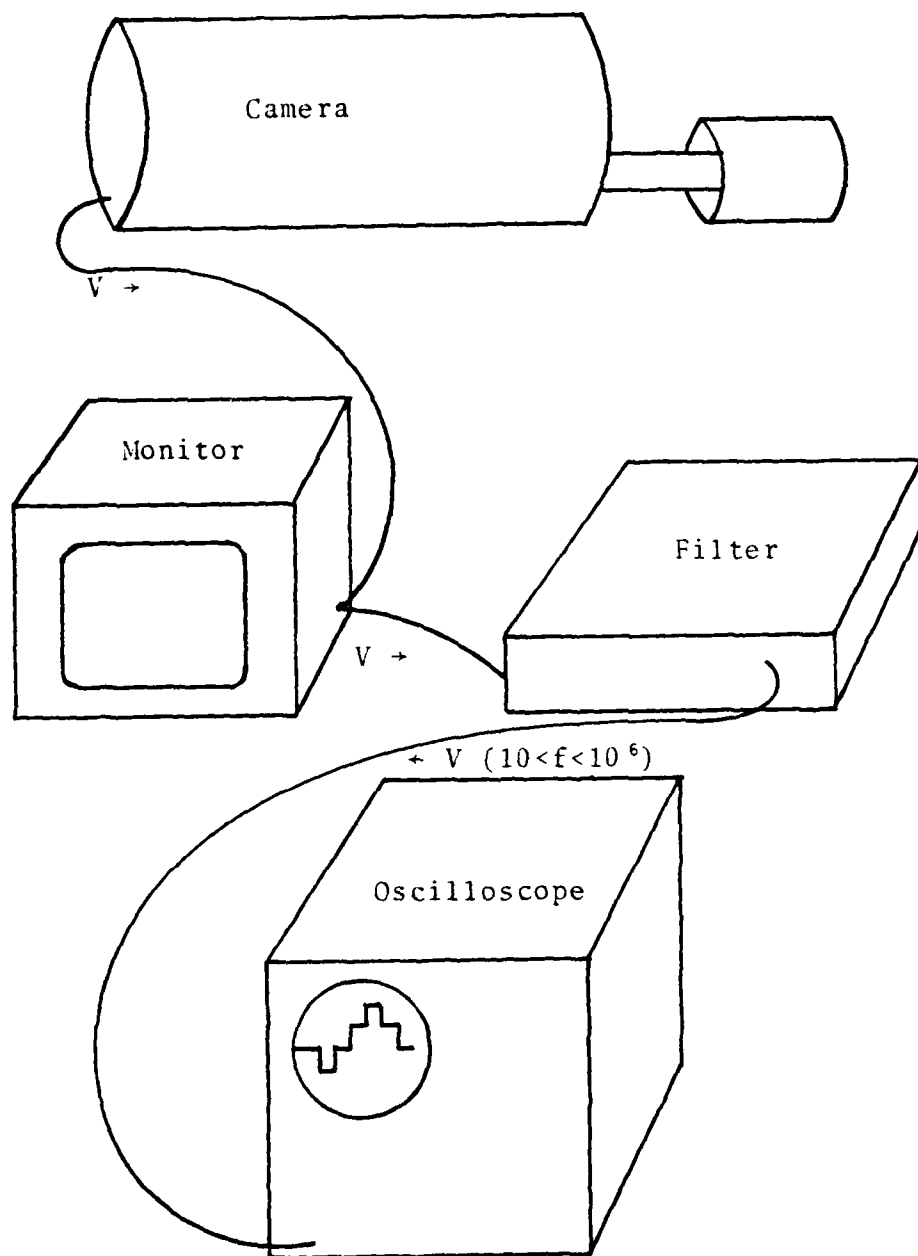


Fig. 4. System Arrangement

Angstroms and cut off at about 8000, it was designed for the visible portion of the spectrum only. A typical spectral response curve for this type tube is included in Appendix A.

The camera used a standard television raster with a line repetition frequency of 525 per frame at a frame rate of 1/30 sec. for a frequency of 15,750 Hz. The signal was a FCC Standard Picture Waveform. Because most prominent features of the local terrain (horizon, tree lines, etc.) exhibited lines of contrast in the nearly horizontal plane, the camera was mounted in a fabricated support tube and rotated 90 degrees (so that it was lying on its side) in order for the horizontally scanning television to scan across the lines of contrast; a single line of the raster would then be looking vertically in the physical region of interest and a distinct contrast line would be evident in the signal. Figure 5 shows the camera in its mount.

Once the camera was set up, properly focused, and calibrated, all of the controls (target, beam, and focus) were never again used; because the power switch was part of the dual purpose Beam/On-off control, power to the unit was switched at the plug.

The vidicon signal current is a function of illumination and target voltage. This camera was designed with a device (Automatic Target Control - ATC) that would produce an equivalent decrease in target voltage with an increase in

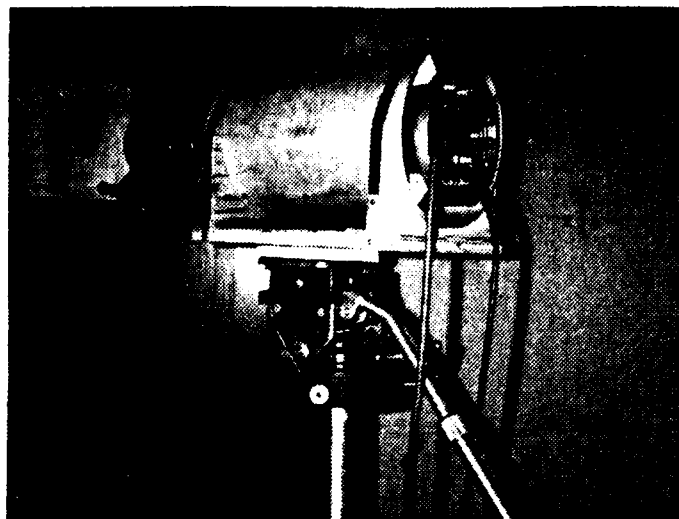


Fig. 5. The Camera

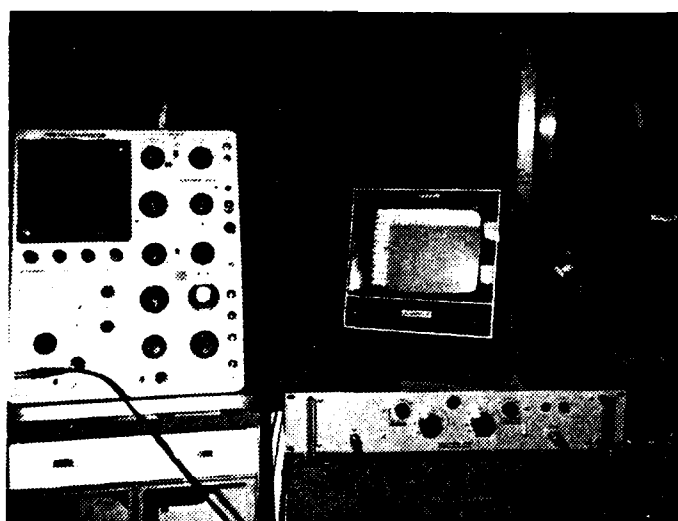


Fig. 6. The Electronics

target illumination in order to get a constant signal output from the camera. This was accomplished by inserting a very large resistor in series with the target voltage supply (V_o , section II.C.) which caused a voltage drop with increased signal resulting overall in a decrease in target voltage and a net decrease in signal until steady state was achieved. This feature would have made all measurements invalid because the voltage was what was measured; the ATC feature was removed by shorting the large resistor in accordance with [2], thus providing only manual target control.

B. THE ELECTRONICS

The electronic components were a KROHN-HITE Model 3100R active filter and a TEKTRONIX Type 585A oscilloscope with a Type 86 Plug-in Unit. The filter was placed in series between the camera video output and the oscilloscope input and adjusted to act as a 10Hz to 1MHz bandpass filter to reject noise. The oscilloscope has a dual time base - one circuit (Time Base B) was adjusted to provide a time delay prior to triggering the second circuit (Time Base A). The display was then an expanded portion of the Time Base B sweep. The oscilloscope was adjusted to pick out one video line at a selected distance from the start of the raster by triggering the delay on the vertical sync pulse which was present at the end of each scan, and triggering

the expanded sweep on the horizontal sync pulse present at the end of each line. Delay Time Monitor (DTM) was the scope adjustment for varying the length of time delay.

Appendix B contains specifics of the oscilloscope adjustments and Fig. 6 shows the physical electronic arrangement. Specifics on the operation of this oscilloscope are contained in its instruction manual [11].

C. THE CALIBRATION UNIT

It was intended that the camera-scope system be used to study contrast and visibility and the effects of the atmosphere; initially, however, it was necessary to examine the characteristics and response of the system under controlled conditions in order to understand the output. A calibration unit was designed and fabricated around the parameters of the camera.

With the camera set to its longest focal length (90 mm.), the minimum distance at which the system could focus was determined to be 138 cm.; the diameter of the field of view at this distance was determined to be approximately 20 cm.

A light-tight enclosure (Fig. 7) was then fabricated of 12 inch ducting, painted flat black on the interior, with end closures. A smaller tube was then fitted to the camera lens and inserted in the viewing end of the tube (to form a

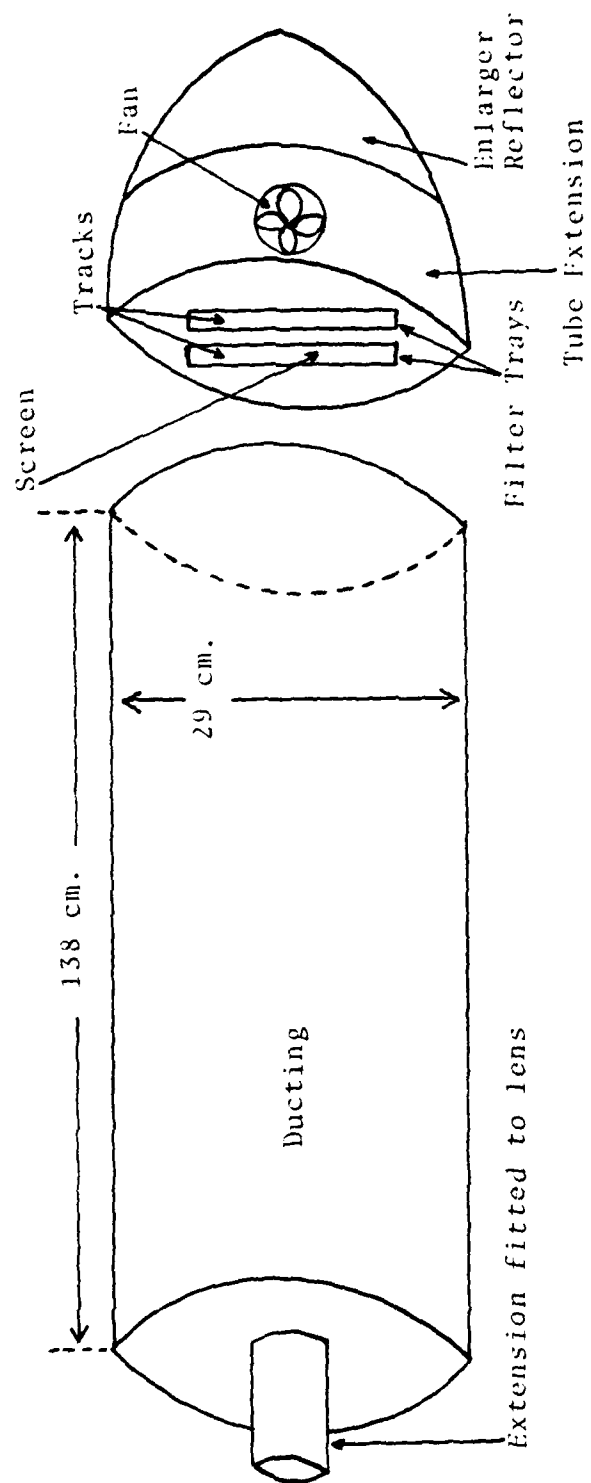


Fig. 7. The Calibration Tube

seal between lens and tube with black neoprene material used to make it flexible but tight). Into the object end of the tube was fitted the light unit which consisted of a photographic enlarger reflector and bulb, a cooling fan, and a ground glass screen which provided a uniform source of illumination. It was necessary to cool the interior of the light unit because it was completely enclosed, so a fan and vent were installed in the tube extension between the reflector and screen which created a heat removing flow of air behind the screen. The portion of the calibration tube between the camera lens and the screen was completely enclosed so that there were no light leaks or any turbulence. Figures 8, 9 and 10 are photos of the calibration unit.

Fitted to the front of the ground glass screen was a pair of metal trays, hinged at the bottom, into which fit filters (Fig. 11); it was hinged and a hand access was provided in the side of the unit to permit changing the filters without separating the pieces of the unit and losing alignment. The regions of the screen visible to the camera through the filter trays have been designated "tracks"; Track A was on the left physically and on the bottom for the camera because it was rotated 90 degrees in its mount, thus allowing the camera to scan along a track.

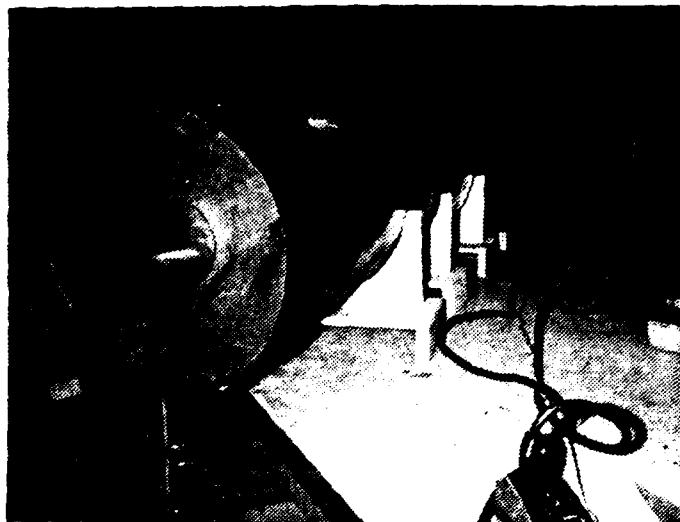


Fig. 8. Calibration Tube (Camera End)

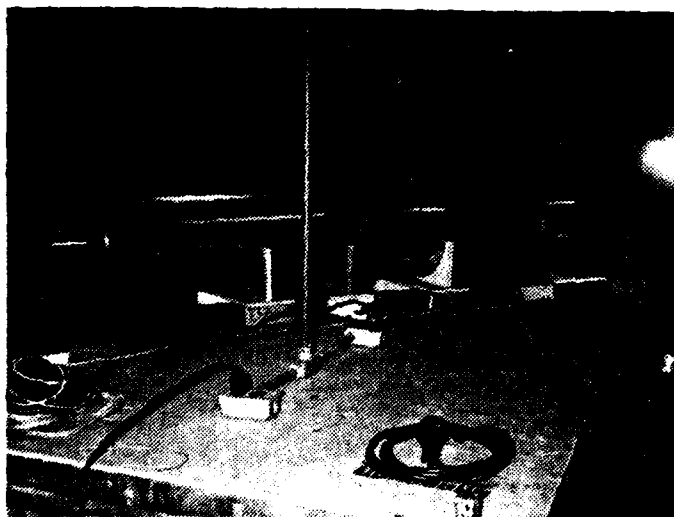


Fig. 9. Calibration Tube (Side View)

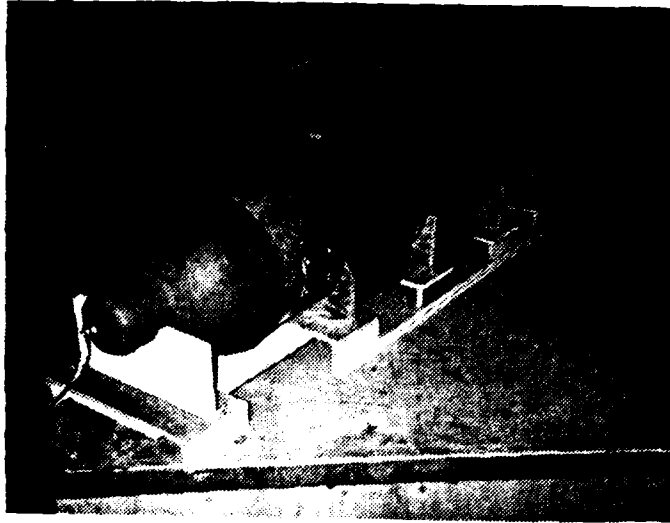


Fig. 10. Calibration Tube (Source End)

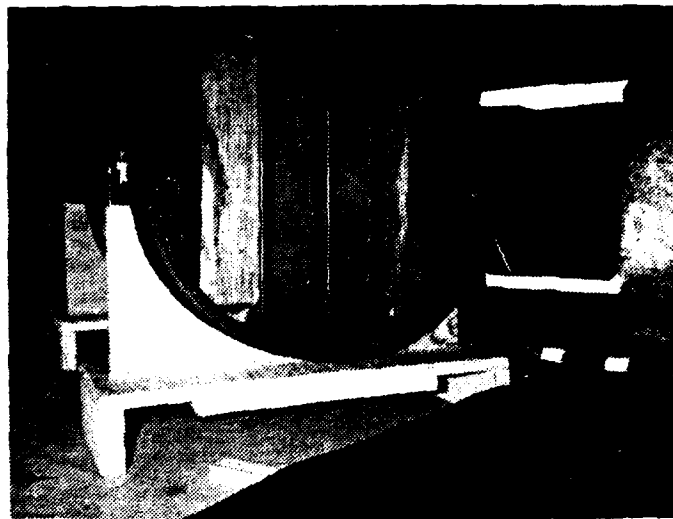


Fig. 11. Screen and Filter Trays

IV. PROCEDURE AND RESULTS

A. PRELIMINARY

The preliminary portion of this experiment was designed to develop a basic understanding of the camera system, the oscilloscope and their output. The object used was a large, flat, black non-reflecting board (black cloth on a 4x8 ft. sheet of plywood) upon which white striping was fastened; the board was placed 3 meters from the camera and the end of one stripe obscured by black cloth so that the scene in Fig. 12 was the field of view. The ATC was still connected, the filter was not yet installed and the output exhibited a lot of noise.

Figure 13 shows an entire scan, all lines between top and bottom in the field of view compressed into the display. The shadow which appears at 3.5 cm. from the beginning of the display is the top of the white line (point B, Fig. 12) while the confused signal at 0.8 cm. above "black" is the black background plus noise; Fig. 14 spreads the display out in the region where the shadow began - the individual lines can now be discriminated; Fig. 15 isolates one line, clearly showing the return from the white line (plus noise). Figure 16 is a sketch of the output (Fig. 15) delineating the features shown.

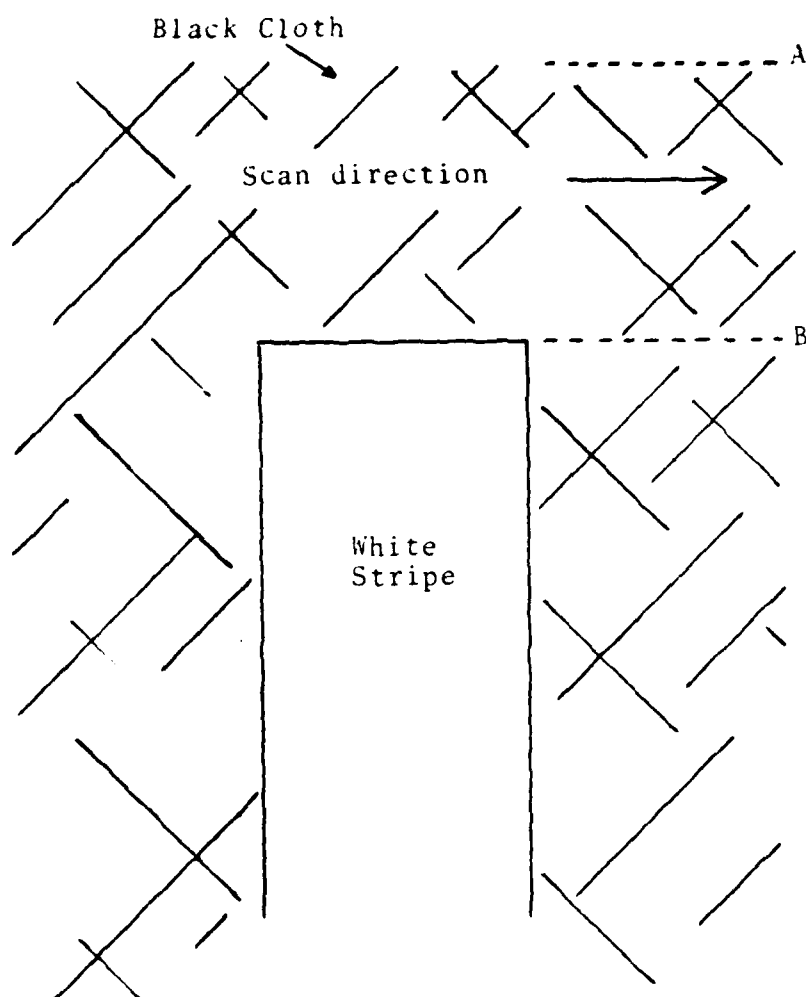


Fig. 12. Laboratory Object Scene

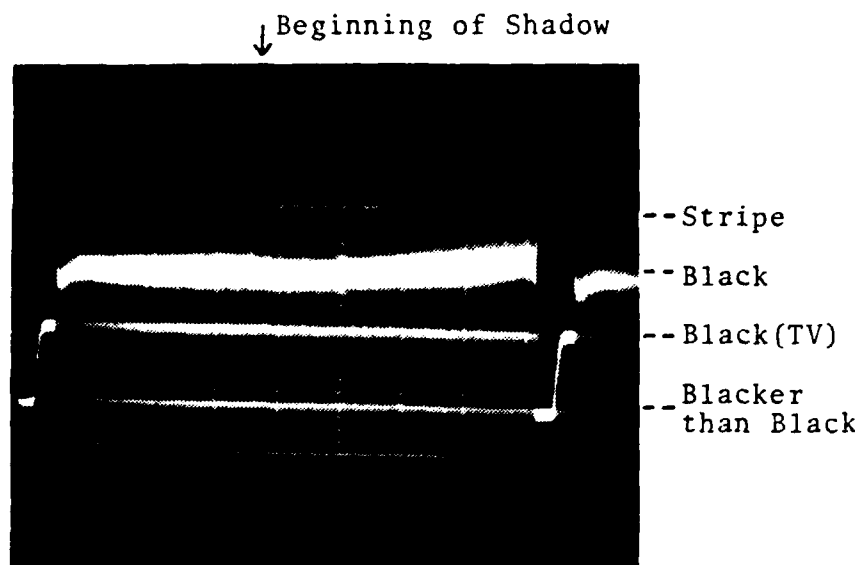


Fig. 13. Lab Object - Entire Scan

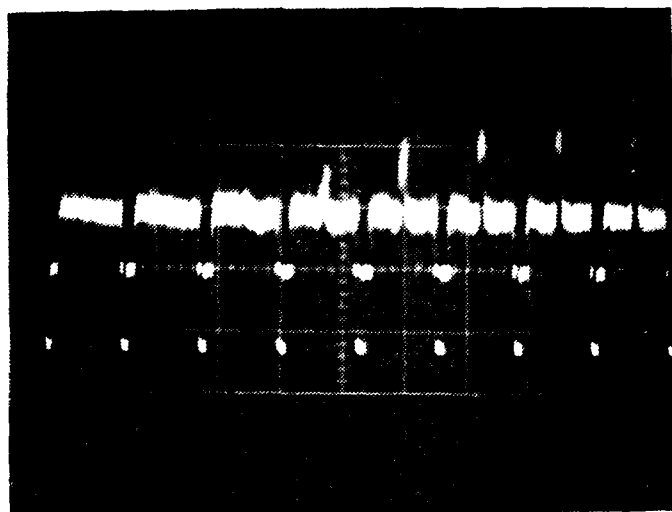


Fig. 14. Lab Object - 8 Lines

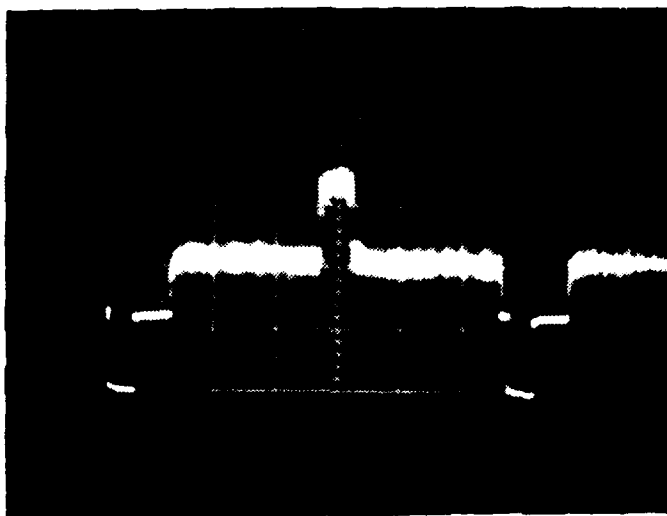


Fig. 15. Lab Object - Single Line

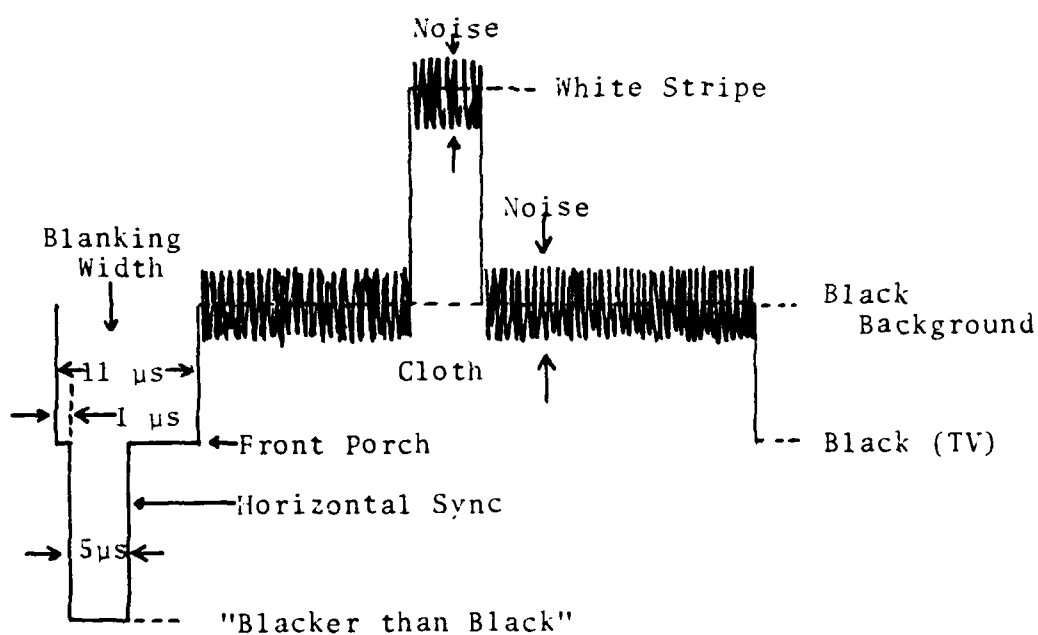


Fig. 16. Single Line Sketch

Once the signal from a single line was recovered, the problem then became to determine how the height of test signal above a reference varied under different conditions. The initial test consisted of varying the distance from which the white stripe was irradiated by an incandescent source (desk lamp) and measuring the reflected result at the oscilloscope; the data was too crude to be of value and it was assumed also that the ATC had performed as designed and made the data meaningless. By the time the ATC was disconnected, the analysis of section II.C had been performed obviating the need for this particular experiment.

Data was then taken to correlate the position in the field of view (data refers to the monitor position) of an object with the appearance of the corresponding signal on the scope. This was accomplished by placing a prominent object (a stanchion on the roof) in the field of view against the sky and noting the appearance of an edge on the monitor and on the scope; by varying the Delay Time Multiplier (DTM), the line could be picked out (zero delay time refers to the start of the scan) at which the effect of the edge was just evident. Once the line was determined, the start of the effect was noted as a distance from the beginning of the line on the scope. The corresponding monitor data was recorded relative to the left edge of the screen (Lateral) or the bottom (Vertical). Figures 17 and 18 are the result

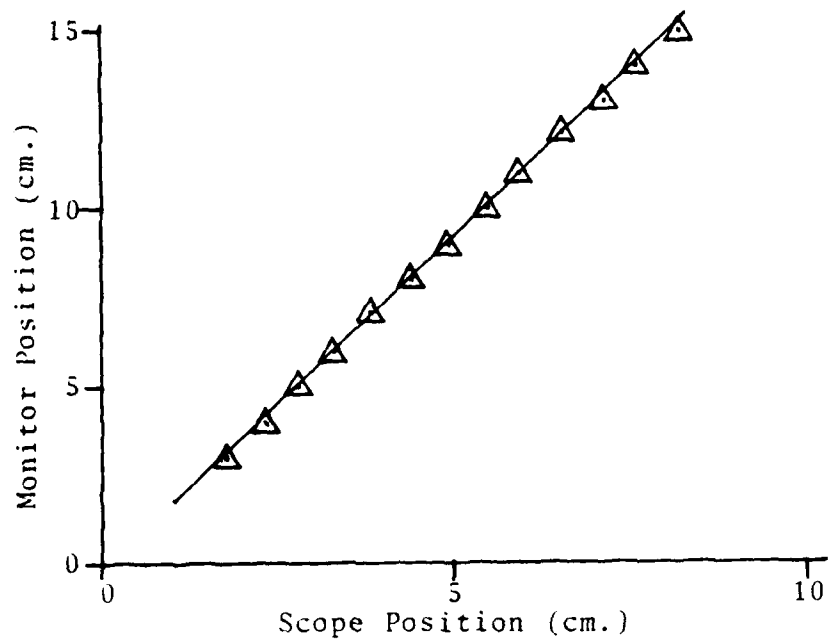


Fig. 17. Lateral Monitor-Scope Correlation

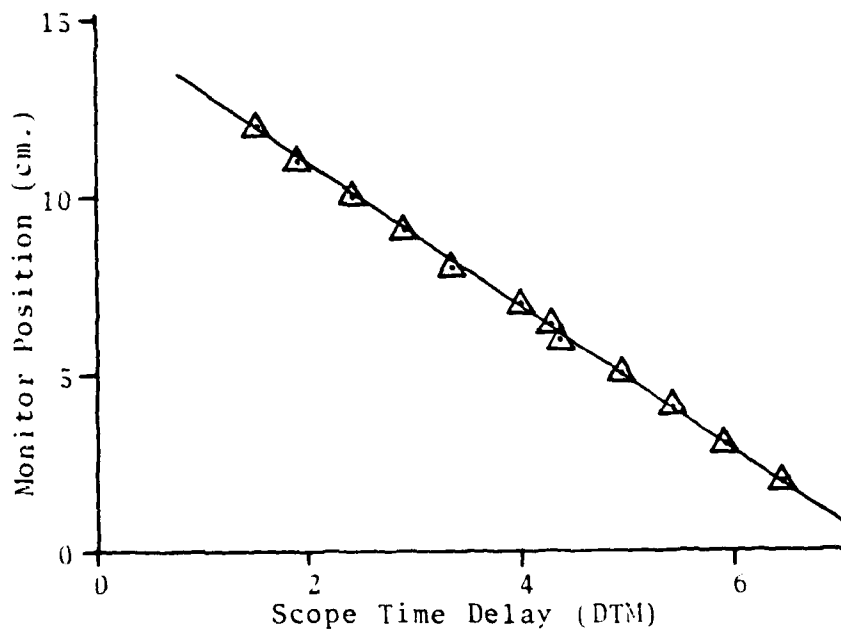


Fig. 18. Vertical Monitor-Scope Correlation

and allow the electronic location of an object of interest on the oscilloscope once its monitor position is measured and vice versa. The data for all experimental plots is contained in Appendix C.

B. CALIBRATION

With the active bandpass filter installed in the system and the ATC disconnected, the camera was then rotated 90 degrees (so that it scanned in the vertical direction physically) and fixed to the calibration tube and the system activated. With no filters installed in front of the screen, the two basically rectangular tracks appeared to have uniform intensity on the monitor, but Figs. 19 and 20 (scans down the tracks) show that the intensity displayed was not a straight flat line, but slightly concave down for both tracks; the intensity appeared to be reasonably uniform over the beginning of the line, but tailed off drastically at the end. Neutral density filters were then placed side by side in the trays in front of the screen (with "light leaks" between filters); Figs. 21 and 22 were the result, exhibiting the same nonlinearity as their respective non-filtered tracks but also showing different levels of intensity as expected of a variety of filters with different densities.

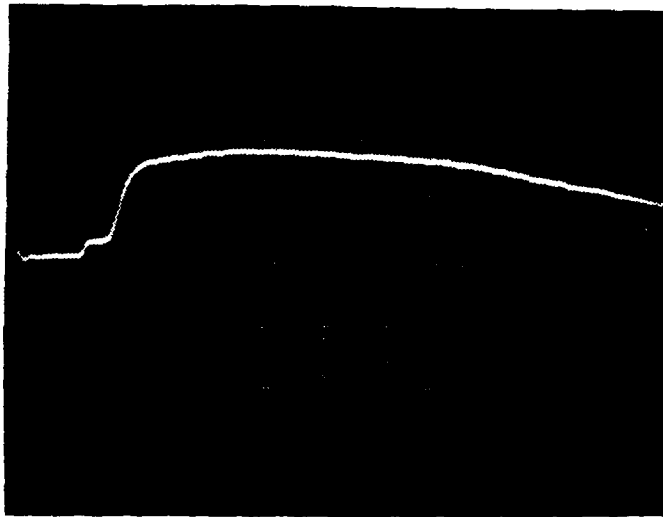


Fig. 19. Screen w/o Filter - Track A

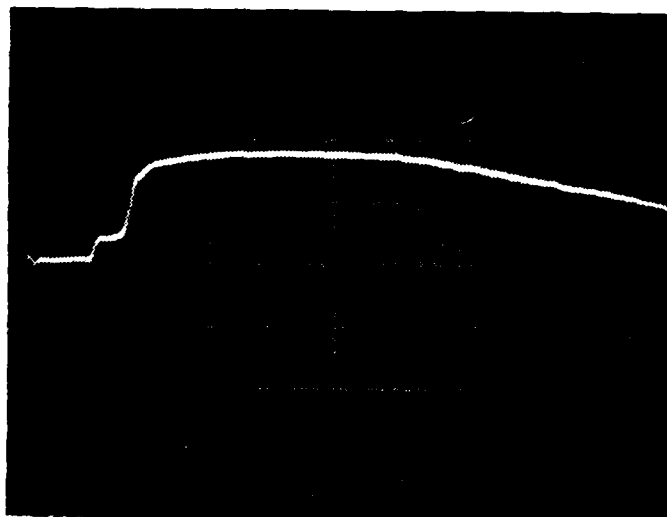
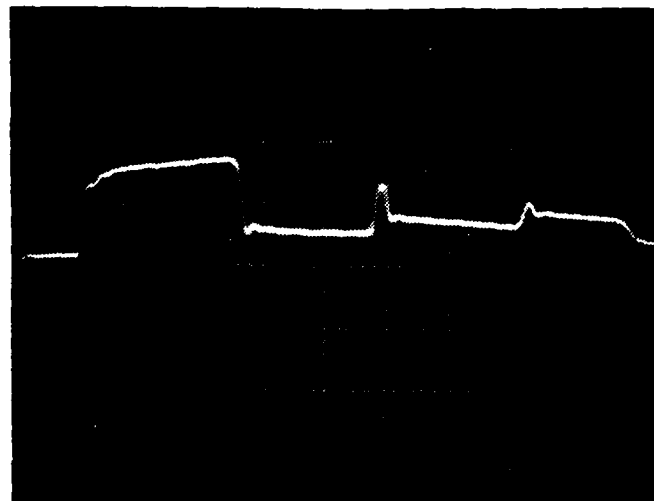


Fig. 20. Screen w/o Filter - Track B



End | None | ND 2 | ND 1 | ND .5 |

Fig. 21. Screen with Filters - Track A

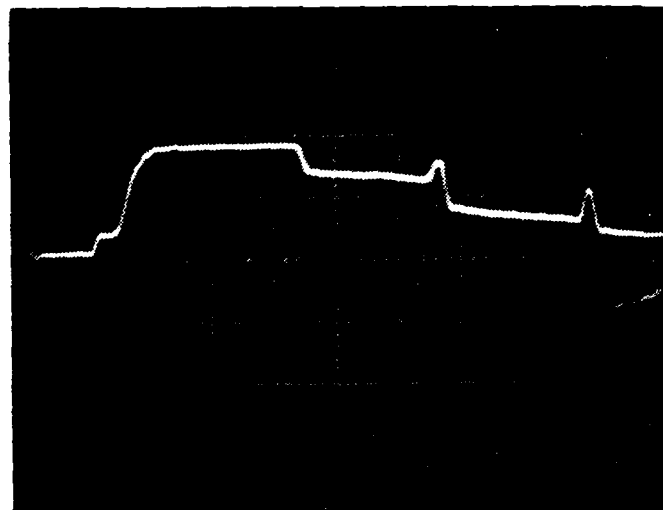
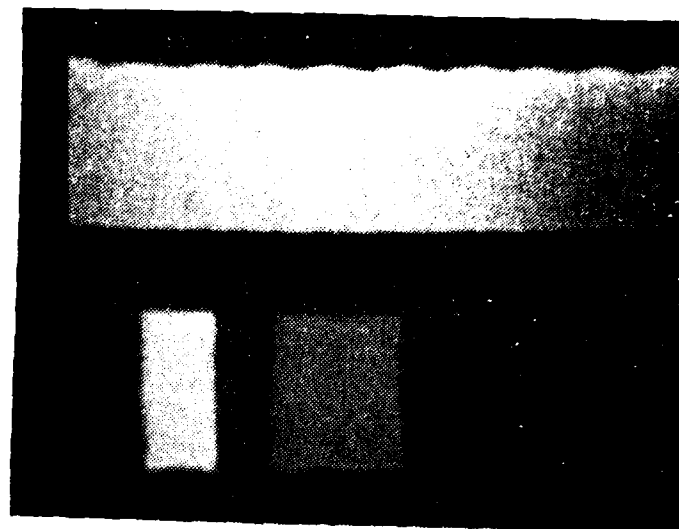


Fig. 22. Screen with Filters - Track B

Figure 23 shows a picture of the monitor with one track not obscured while filters were placed in the second with flat black opaque separators; Fig. 24 is the oscilloscope result.

The system had then proven (qualitatively) that it could discriminate a change in intensity, but that either the calibration screen or the camera system or both were not uniform across the area of interest, also the response of a single spot on the detector to changes in intensity was not known (verification of the previous analysis). Useful outside world data could only be taken once the system errors were identified and properly corrected.

First, the uniformity of the screen was checked for each track; this was accomplished by covering the screen except for one 1/8 inch slit and repositioning the camera system on the slit each time it was moved to preclude introduction of error from the camera. The slit was kept centered in the monitor by ensuring that it was always contained within a frame taped to the monitor; the slit was sequentially shifted to 15 different positions (each $\frac{1}{2}$ inch apart) along each track. The results are depicted in Figs. 25 and 26; excluding the extreme sides of the tracks (slits #1,2,14,15), the screen is basically uniform across its width. Track to track data cannot be correlated because it was taken on different days, but that is inconsequential because only along the raster line is this calibration critical.

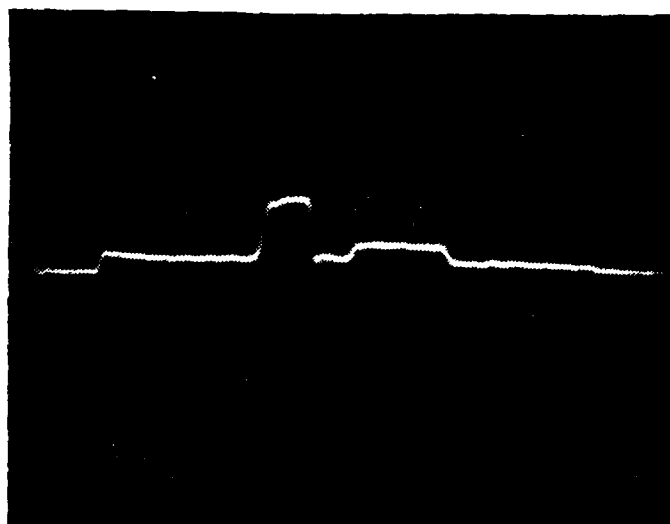


Track B
w/o filters

Track A
with filters

Black | None | | ND 1 | | ND 2 |

Fig. 23. Monitor - Screen with Filters



Black | None | ND 1 | | ND 2 |

Fig. 24. Signal of Monitor Scene - Track A

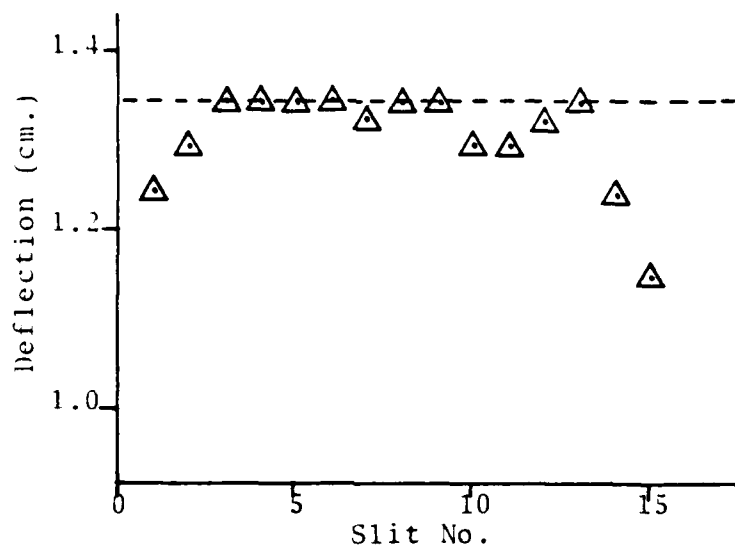


Fig. 25. Deflection vs Slit No. - Track A

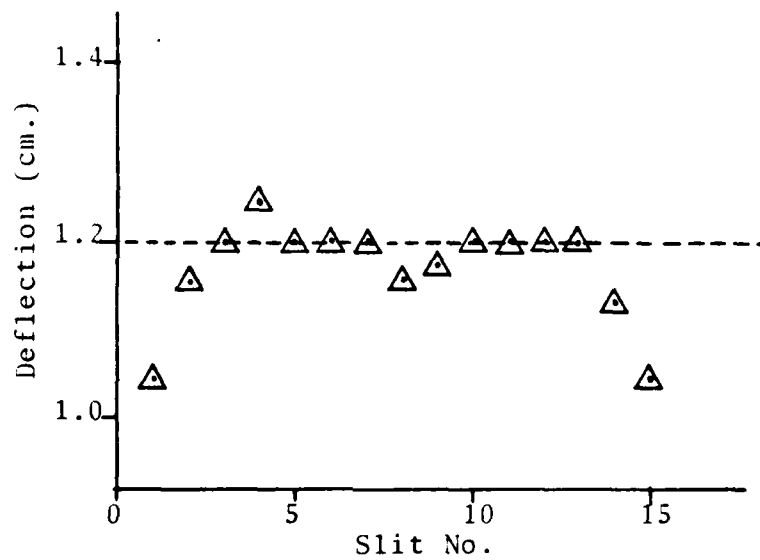


Fig. 26. Deflection vs Slit No. - Track B

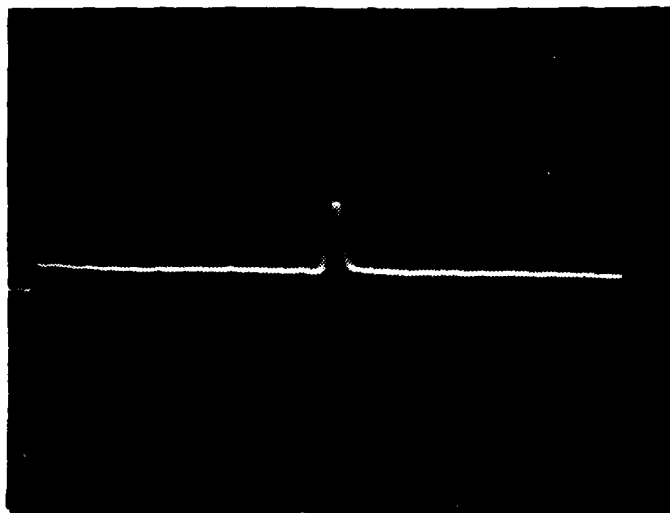


Fig. 27. Output from Single Slit

Figure 27 shows the spike from the slit as it appeared on the oscilloscope.

Next, the camera system field of view was checked by performing the converse experiment; slit #6, Track B was maintained as a permanent target and the image was "driven around the monitor" by altering the camera position. Thus, nonuniformities in the screen would not have caused any error in the readings. A grid of rows and columns each separated by 1 cm. was then superimposed on the monitor. The image of the slit was started at the top left corner and moved laterally across the top row from left to right, then repeated across the next row down, sequentially until deflection data was recorded for each 2-D point on the grid. The data from each column and row was then averaged and the deflection means plotted versus their respective lateral (for column) and vertical (for row) positions. Figures 28 and 29 are plots of the column or row mean deflection versus position; they make it apparent that the detector/camera system can in no way be considered uniform. From left to right a steady and considerable decrease is noted (consistent with that noted in Figs. 19 and 20); from top to bottom it is not as steady, but this is not the critical direction.

Finally, both the position on the screen and the monitor was kept constant and the intensity of the illumination from the single spot was varied by putting different neutral

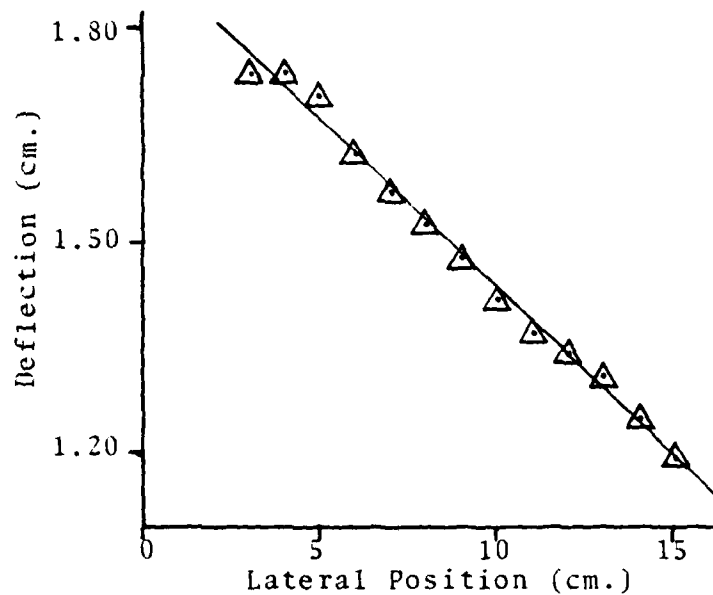


Fig. 28. Deflection Mean (Column) vs Lateral Monitor Position

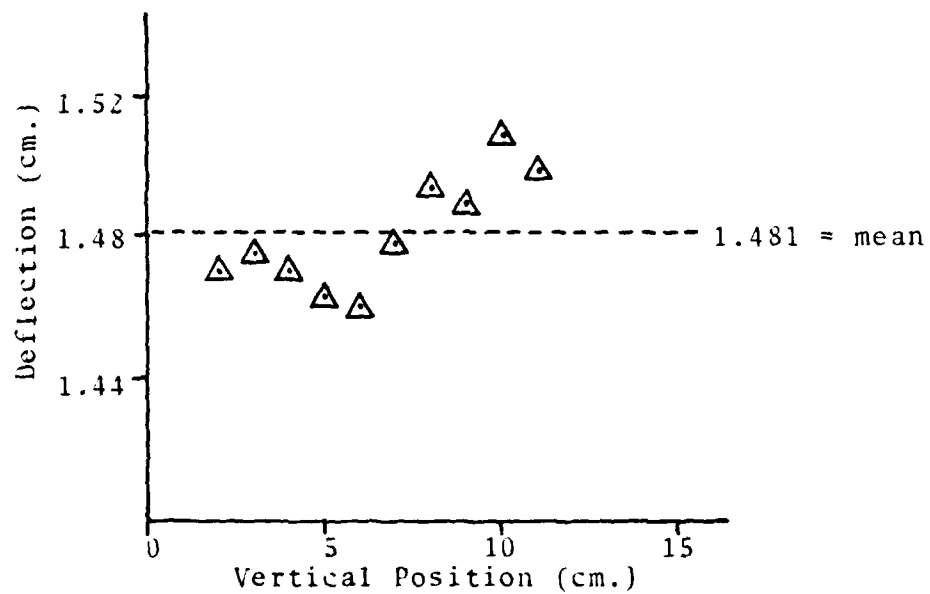


Fig. 29. Deflection Mean (Row) vs Vertical Monitor Position

density filters in the trays; the purpose here was to check system response to changing illumination levels - the essence of contrast determination. Initially (prior to the analysis of Section II.C) it was assumed that the deflection was linearly dependent upon either the transmission coefficient (T) or the neutral density number (ND) where $ND = -\log_{10} T$. Figures 30 and 31 are attempts to fit the deflection data linearly to T and ND; both were unsuccessful so a different approach was chosen.

The analysis of Section II.C postulated that

$$\ln(1-fD) = \sigma^* + gt \quad (22)$$

thus, if f could be determined, the other two constants would become slope and intercept and linear regression of the data would find them. A guess was made of a value for f and the data fitted; then iteratively new guesses were made until a maximum in correlation coefficient was discovered. The data was then plotted along with the line determined by the best linear regression fit (Figs. 32 and 33). A decent fit was discovered in each case, but the values of f were not found to be equal. Two alternative interpretations were evident: (1) The data was accurate implying that the theory was faulty - possibly f could not be regarded as a constant but was in fact a function of T or some other variable; and (2) the theory was correct implying that the data was not accurate enough for confirmation.

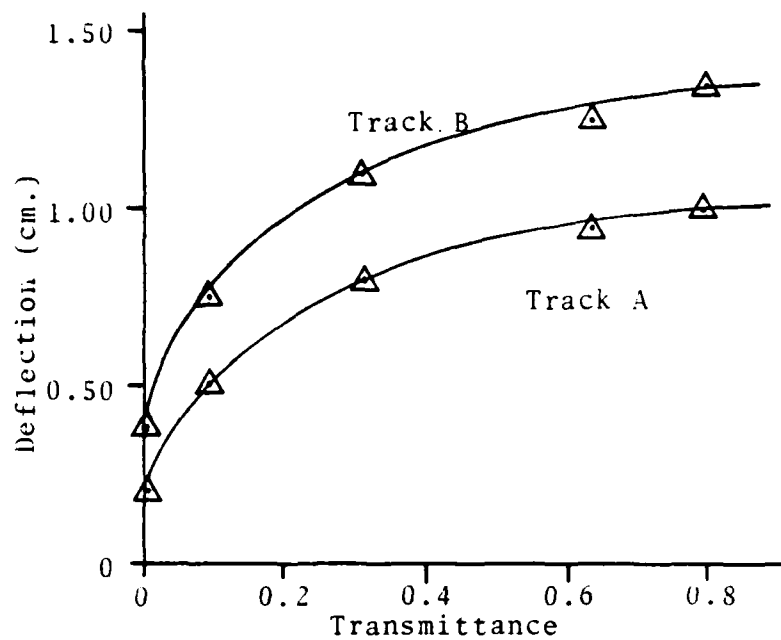


Fig. 30. Deflection vs Transmittance

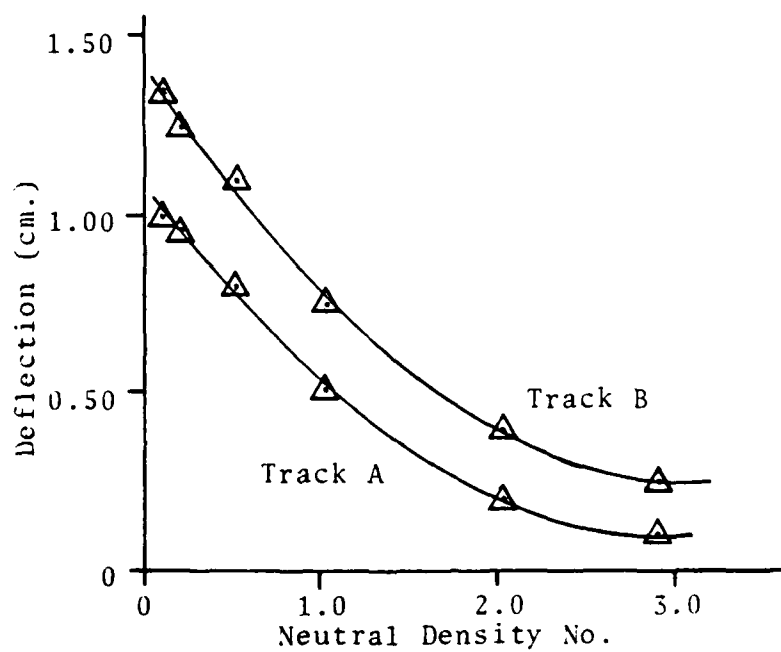


Fig. 31. Deflection vs Neutral Density No.

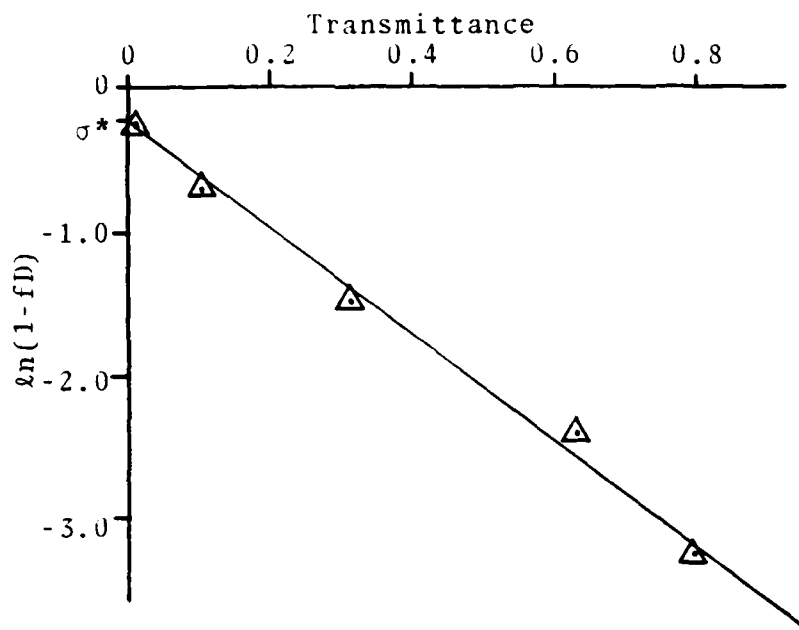


Fig. 32. $\ln(1-fD)$ vs Transmittance - Track A

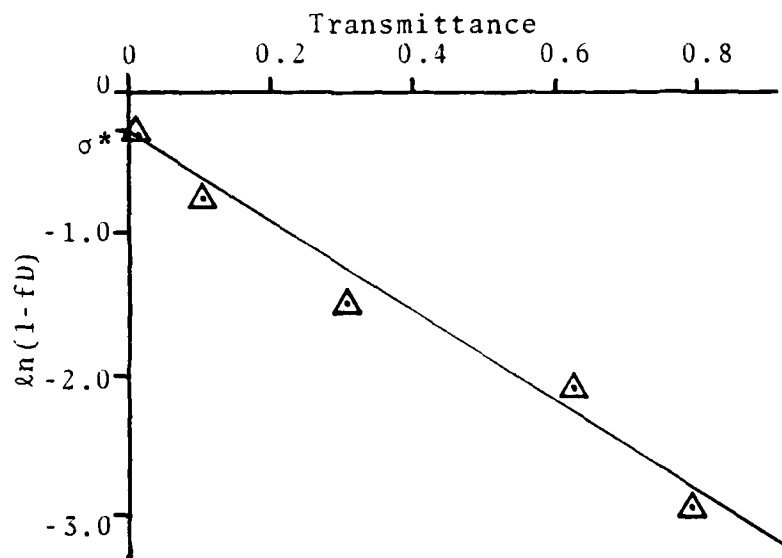


Fig. 33. $\ln(1-fD)$ vs Transmittance - Track B

The foregoing calibration indicates that the system is responsive to changes in intensity, however quantitatively the system characteristics could not yet be determined.

C. TYPICAL SCENE

The purpose behind this investigation, and particularly the calibration, was to develop a system which would determine contrast in the local environment. Although the previous data was somewhat inconclusive, the system was set up to monitor a local area from the roof of Spanagal Hall; the area chosen was that around and behind the Monterey Peninsula Airport - a scene with several distinct contrast lines at distances that could be measured should realistic data be taken.

This scene (Fig. 34) included a rather faint (to the naked eye) but distinct sky-hill horizon behind the airport, which was scanned vertically, but this distinct change could not be found on the scope (Fig. 35). It was noted that the exact positioning using Figs. 17 and 18 was very difficult to check because of the lack of sharpness of the trace.

↓ Location and direction of scan



Fig. 34. Photograph of Actual Scene

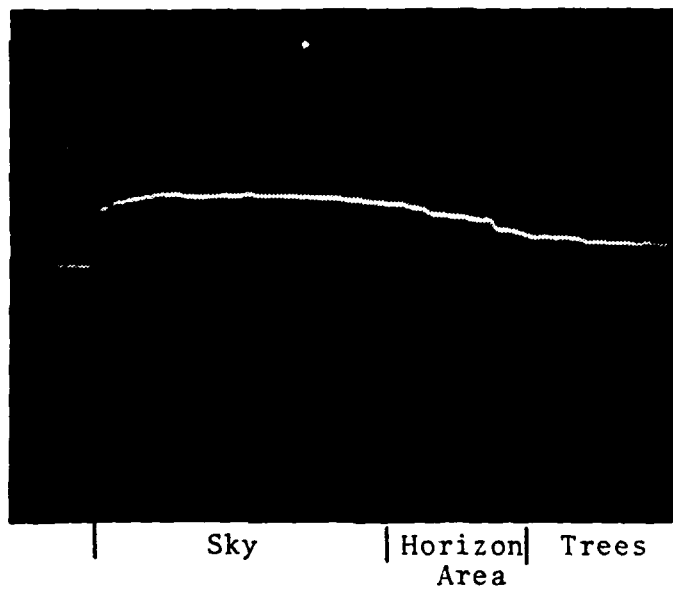


Fig. 35. Output from Horizon Area of Actual Scene

V. CONCLUSIONS AND AREAS FOR FURTHER STUDY

The foregoing results were enlightening. It was discovered that the commercial multi-purpose camera system used for this experiment could discern differences in intensity and consequently contrast; it was possible to measure these differences by analyzing the output from the camera. A derivation of probable system response was made; the data appeared to basically confirm the theory developed; however a constant system function (f) could not be found when the viewing point on the ground glass screen was changed. It is possible that exactly the same pixel on the detector was not used for each data set, wherein a difference between pixels would have precluded determination of a valid and constant f . Figure 28, which showed a decrease in deflection readings as the image was moved from left to right implied an error introduced by the electronics, possibly a scanning electron beam which was accelerating as it moved to the right. Figure 29 showed a difference of 1.6 percent about a mean of 1.481 cm. in a random pattern as the image moved from bottom to top, which implied that the detector was quite uniform from row to row. An analysis was performed of the "interior" area of the monitor which excluded the 6 outer columns and 4 extreme rows; this region was more uniform and should be preferred for analysis.

The system studied was not refined enough to permit quantitative analysis in the local environment. Improvement is necessary in the following: (1) prediction of detector response; (2) correlation between monitor and oscilloscope positions of the signal of interest; and (3) data retrieval - a sampling unit (1S1) is available as an oscilloscope plug-in which could possibly be used as an interface to provide data at a manageable rate to a digital analyzer.

The critical piece of equipment, the vidicon, was not designed for laboratory work and proved to be nonuniform; a better quality and more accurate tube would be beneficial for future work. Vidicons are being developed with a spectral response in the infrared region; a high quality tube of this type would permit work in the near IR.

Once this system is refined, then measurement of visibility with it is possible; furthermore, the system would prove valuable in the determination of atmospheric effects on contrast and visibility.

APPENDIX A OPERATING CHARACTERISTICS OF CAMERA

Scanning:	Random interlace, 2:1, 30 frames 60 fields per sec.
Horizontal Sweep:	15,750 cps
Horizontal Sync and Blanking:	Blanking width 11.3 μ sec, front porch 1.0 μ sec, sync width 5 μ sec
Vertical Sync and Blanking;	Blanking width 1250 μ sec, sync width 200 μ sec
Signal to Noise Ratio:	Minimum 40:1 peak signal to rms noise with 0.5 fc or more vidicon faceplate illumination
Sensitivity:	Usable picture with scene brightness down to 1.5 fl using f/1.4 lens
Video Bandwidth:	8 Mc \pm 1 db, less than 3 db down at 10 Mc
Light Compensation:	Without adjustment, automatic light compensation will operate over at least a light change ratio of 3000:1 with a video level change not exceeding 2:1

Light Compensation (cont'):

The picture will stabilize
after any light change within
one second.

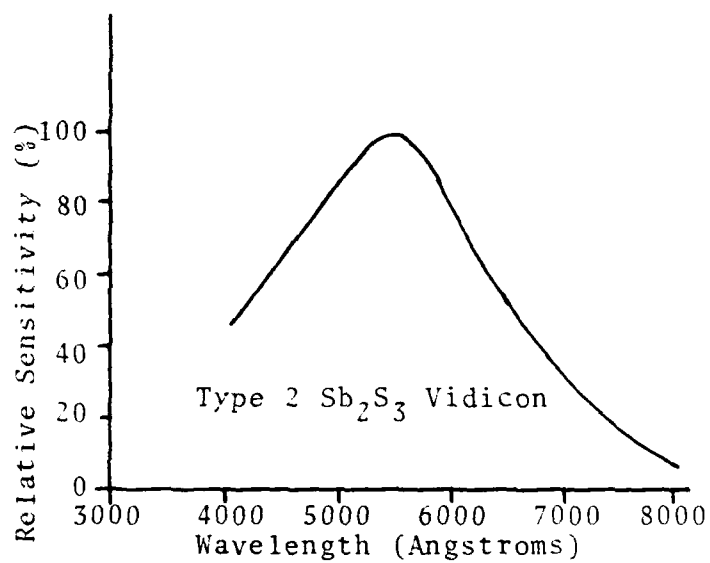


Fig. 36. Image Tube Spectral Response

APPENDIX B OSCILLOSCOPE SETTINGS

To examine the signal on the TEKTRONIX 585A Oscilloscope, the following settings were used:

Time Base A

Trigger Slope: +

Trigger Source: AC

Time/cm: 5 μ sec

Horizontal Display: "A" DLY'D by "B"

Time Base B

Trigger Slope: -

Trigger Source: Line

Time/cm: 2 msec

Delay Time Multiplier: Variable

Amplitude Calibrator: Off

Type 86 Plug-in High-Gain Fast-Rise

Volts/cm: 0.2 x 1

APPENDIX C DATA

<u>Monitor (cm.)</u>	<u>Oscilloscope (cm.)</u>
3	1.80
4	2.35
5	2.80
6	3.30
7	3.80
8	4.40
9	4.90
10	5.45
11	5.95
12	6.55
13	7.15
14	7.70
15	8.20

TABLE I. Monitor Versus Oscilloscope Calibration
Data (Lateral)

<u>Monitor (cm.)</u>	<u>Oscilloscope (DTM)</u>
12.0	1.530
11.0	1.900
10.0	2.412
9.0	2.888
8.0	3.370
7.0	3.955
6.5	4.260
6.0	4.332
5.0	4.900
4.0	5.425
3.0	5.900
2.0	6.432

TABLE II. Monitor Versus Oscilloscope Calibration
Data (Vertical)

<u>Slit No.</u>	<u>Deflection (cm.)</u>	
	<u>Track A</u>	<u>Track B</u>
15	1.15	1.05
14	1.25	1.13
13	1.35	1.20
12	1.33	1.20
11	1.30	1.20
10	1.30	1.20
9	1.35	1.17
8	1.35	1.15
7	1.33	1.20
6	1.35	1.20
5	1.35	1.20
4	1.35	1.25
3	1.35	1.20
2	1.30	1.15
1	1.25	1.05
(Slits 3-13)		
mean	1.337	1.197
std. dev.	.020	.024

TABLE III. Screen Calibration Data

LATERAL POSITION (cm.)

	3	4	5	6	7	8	9	10	11	12	13	14	15
11	1.65	1.70	1.70	1.65	1.55	1.55	1.55	1.50	1.42	1.36	1.35	1.30	1.20
10	1.75	1.75	1.70	1.62	1.55	1.52	1.50	1.48	1.42	1.40	1.37	1.32	1.22
9	1.73	1.73	1.70	1.65	1.60	1.50	1.45	1.41	1.40	1.35	1.32	1.30	1.20
8	1.75	1.75	1.70	1.60	1.58	1.53	1.46	1.41	1.40	1.38	1.35	1.30	1.20
7	1.75	1.74	1.68	1.60	1.56	1.52	1.50	1.40	1.35	1.34	1.32	1.25	1.20
6	1.75	1.70	1.64	1.60	1.57	1.55	1.50	1.40	1.35	1.34	1.22	1.20	1.16
5	1.70	1.75	1.68	1.60	1.58	1.53	1.45	1.40	1.35	1.32	1.30	1.20	1.16
4	1.75	1.75	1.65	1.61	1.58	1.52	1.48	1.40	1.37	1.35	1.30	1.20	1.16
3	1.75	1.75	1.73	1.65	1.60	1.55	1.45	1.36	1.34	1.32	1.30	1.20	1.19
2	1.76	1.75	1.73	1.65	1.55	1.50	1.42	1.40	1.35	1.30	1.28	1.23	1.20

Deflection (cm.) Versus Monitor Position

TABLE IV. Raw Detector Calibration Data

VERTICAL POSITION (cm.)

Position (cm.)		Deflection (cm.)			
		Interior only			
		<u>mean</u>	<u>std. dev.</u>	<u>mean</u>	<u>std. dev.</u>
(Lateral)					
	3	1.734	.034		
	4	1.737	.021		
	5	1.691	.030		
	6	1.623	.024	1.610	.020
	7	1.572	.019	1.578	.013
	8	1.527	.019	1.525	.016
	9	1.476	.037	1.473	.023
	10	1.416	.042	1.403	.005
	11	1.375	.032	1.370	.024
	12	1.346	.030	1.347	.020
	13	1.311	.043		
	14	1.250	.050		
	15	1.189	.021		
(Vertical)					
	11	1.498	.161		
	10	1.508	.165		
	9	1.488	.178	1.480	.110
	8	1.493	.175	1.480	.090
	7	1.478	.183	1.467	.104
	6	1.460	.196	1.473	.108
	5	1.463	.193	1.461	.111
	4	1.471	.194	1.473	.103
	3	1.476	.207		
	2	1.471	.201		

TABLE V. Reduced Detector Calibration Data

<u>T</u>	<u>ND</u>	Deflection (cm.)	
		<u>Track A</u>	<u>Track B</u>
.794	0.10	1.00	1.35
.631	0.20	0.95	1.25
.309	0.51	0.80	1.10
.098	1.01	0.52	0.75
.009	2.03	0.20	0.38
.001	2.90	0.10	0.25

Note: T was derived from knowledge of ND

TABLE VI. Deflection Versus Filter Data

BIBLIOGRAPHY

1. Businger, J.A. and Fleagle, R.G., An Introduction to Atmospheric Physics, Academic Press, 1963.
2. Diamond Electronics, Instructions Model ST-1 Camera System, ed. II, rev. October 1967.
3. Duntley, S.Q., "The Reduction of Apparent Contrast by the Atmosphere," J Opt. Soc. Am., v. 38, pp. 179-191, February 1948.
4. Duntley, S.Q., "The Visibility of Distant Objects," J Opt. Soc. Am., v. 38 pp. 237-249, March 1948.
5. Electro-Optics Handbook, Technical Series EOH-11, RCA, 1974.
6. Huschke, R.E., Glossary of Meteorology, AMS, Boston, 1959.
7. Johnson, J.C., Physical Meteorology, Technology Press of M.I.T. and Wiley, 1954.
8. McCartney, E.J., Optics of the Atmosphere, Wiley, 1976.
9. Middleton, W.E.K., Vision Through The Atmosphere, Univ. of Toronto Press, 1952.
10. Stark, H. and Tuteur, F.B., Modern Electrical Communications Theory and Systems, Prentice-Hall, 1979.
11. Tektronix, Inc., Instruction Manual Type 585A Oscilloscope, Tektronix, Inc. 1966.

INITIAL DISTRIBUTION LIST

	No. Copies
1. Defense Technical Information Center Cameron Station Alexandria, Virginia 22314	2
2. Library, Code 0142 Naval Postgraduate School Monterey, California 93940	2
3. Department Chairman, Code 61 Department of Physics and Chemistry Naval Postgraduate School Monterey, California 93940	2
4. Professor E. C. Crittenden Jr., Code 61ct Department of Physics and Chemistry Naval Postgraduate School Monterey, California 93940	2
5. Professor A. W. Cooper, Code 61cr Department of Physics and Chemistry Naval Postgraduate School Monterey, California 93940	1
6. LCDR Richard William Havel 449 Branch Avenue Little Silver, New Jersey 07739	1

